EISSN: 2231-0916 doi: 10.14202/vetworld.2026.4970-4980 OPEN ACCESS

Veterinary World

RESEARCH ARTICLE

Sodium caseinate-induced progressive testicular amyloidosis in adult male rats: Histopathological, histochemical, and immunohistochemical characterization

Mohammed A. Al-Salih, Sanaria H. Al Katy, A. M. Al-Saidya and Hana Kh. Ismail

Department of Pathology and Poultry Diseases, College of Veterinary Medicine, University of Mosul, Mosul, Iraq.

ABSTRACT

Background and Aim: Amyloidosis is characterized by extracellular deposition of misfolded fibrillar proteins that can disrupt tissue architecture and function. Although amyloid deposition has been extensively investigated in several organs, testicular involvement remains poorly characterized. This study investigated whether sodium caseinate (CasNa) administration induces progressive amyloid deposition in the testes of adult male rats and characterized the associated histopathological, histochemical, and β-amyloid (Aβ) immunohistochemical changes.

Materials and Methods: Twenty healthy adult male Albino Wistar rats (*Rattus norvegicus*) were randomly allocated to control and treatment groups (n = 10/group). Controls received 3.0 mL/kg intraperitoneal distilled water, whereas treated rats received 3.0 mL/kg body weight of 8% (w/v) CasNa. Five rats from each group were euthanized on days 25 and 60. Testicular tissues were evaluated using hematoxylin and eosin staining, histomorphometric measurement of seminiferous tubule diameter, and Congo red staining for amyloid-associated deposits. Immunohistochemistry was performed to assess Aβ immunoreactivity.

Results: CasNa administration induced progressive testicular lesions. On day 25, treated rats showed seminiferous tubule alterations, vascular congestion and vasculitis, germinal epithelial detachment, impaired spermatogenesis, and proteinaceous deposition in the interstitium. By day 60, severe necrosis, loss of normal testicular architecture, and mononuclear inflammatory cell infiltration were evident. Seminiferous tubule diameter decreased significantly in treated rats, with a greater reduction on day 60 (241.4 ± 9.664) than on day 25 (301.7 ± 4.597) ($p < 0.0001$). Congo red staining demonstrated extracellular amyloid-associated deposits predominantly in the interstitial tissue and along seminiferous tubule basement membranes. Aβ immunoreactivity was absent in controls but was moderate on day 25 (30.42 ± 6.870) and intense on day 60 (61.34 ± 6.870) in treated rats. Immunoreactivity increased significantly in both treated groups compared with controls and was significantly greater on day 60 than on day 25 ($p < 0.0001$).

Conclusion: Chronic CasNa administration induces progressive testicular amyloid-associated deposition, substantial structural damage, and increasing Aβ immunoreactivity in adult male rats. These findings support this experimental model for investigating testicular amyloidosis; however, Congo red staining and Aβ immunoreactivity alone don't conclusively establish the biochemical identity of the deposited protein. Therefore, complementary molecular and biochemical approaches are required to confirm the identity of the deposited amyloid protein and determine its effects on male reproductive function.

Keywords: amyloid deposition, β-amyloid, Congo red, histopathology, immunohistochemistry, sodium caseinate, testicular amyloidosis, *Rattus norvegicus.*

INTRODUCTION

Amyloidosis is characterized by the extracellular deposition of insoluble fibrillar proteins, termed amyloid, in tissues and organs, disrupting tissue architecture and impairing organ function [1, 2]. Amyloid fibrils originate from normally soluble precursor proteins that misfold, aggregate, and deposit in the extracellular space and typically have a β-sheet-rich structure [3]. Although the effects of amyloid deposition in organs such as the heart and kidneys [4], liver [5], and peripheral nerves [6] are well recognized, experimental studies of amyloidosis have predominantly focused on systemic models. Traditionally, researchers have induced amyloid A (AA) amyloidosis in mice by repeatedly administering casein, which produces sustained inflammation and increases serum amyloid

Corresponding Author: Sanaria H. Al Katy
E-mail: Sanariaalkaty@uomosul.edu.iq

Received: 24-06-2026, **Accepted:** 07-10-2026, **Published online:** 04-11-2026

Co-authors: MAA: mohammed.aadnan@uomosul.edu.iq; AMA: al2011saidya@uomosul.edu.iq; HKI: hanakhaleel@uomosul.edu.iq

How to cite: Al-Salih MA, Al Katy SH, Al-Saidya AM, Ismail HK. Sodium caseinate-induced progressive testicular amyloidosis in adult male rats: Histopathological, histochemical, and immunohistochemical characterization. Vet World, 2026, 19(11): 4970–4980.

Copyright: Al-Salih *et al*. This article is an open access article distributed under the terms of the Creative Commons Attribution 4.0 International License (https://creativecommons.org/licenses/by/4.0/).

A (SAA), ultimately promoting amyloid fibril deposition in various organs [7].

Sodium caseinate (CasNa), a bovine milk-derived protein salt, represents an experimental stimulus of interest in this context. Although primarily used as a nutritional milk protein derivative, CasNa has also been reported to modulate immunological and inflammatory responses and mobilize hematopoietic stem cells in mice [8, 9]. However, its potential to promote amyloid accumulation in the testis following prolonged inflammatory stimulation remains insufficiently investigated. Persistent inflammation and increased production of inflammatory mediators can promote abnormal processing and misfolding of soluble precursor proteins, facilitating their conversion into β-sheet-rich structures. Progressive aggregation and accumulation of these proteins can then lead to extracellular deposition of insoluble amyloid fibrils, with potential structural and functional consequences for affected tissues [10, 11].

Amyloid deposition may also be localized to specific tissues. Localized amyloid deposits are important pathological components of several diseases, including Parkinson's disease, Alzheimer's disease, and type 2 diabetes mellitus, although these disorders are not generally classified as amyloidoses because amyloid deposition represents only one component of their overall pathological processes [12]. Despite increasing knowledge of amyloid-associated disorders, relatively little is known about the consequences of amyloid deposition within the male reproductive system, particularly the testis.

Testicular amyloidosis is uncommon; nevertheless, available clinical evidence indicates that substantial amyloid deposition may be associated with hypogonadism, impaired spermatogenesis, macroorchidism, and compromised reproductive function. Testicular involvement has been reported in approximately two-thirds of male patients with hereditary amyloidosis associated with the apolipoprotein A-I Leu75Pro mutation, in some cases representing the first or only affected organ. Histological examination demonstrated extensive amyloid deposition associated with azoospermia or severe oligospermia [13]. Testicular amyloidosis has also been associated with impaired testicular function and reduced fertility [14]. Collectively, these observations indicate that amyloid deposition can directly affect the testis and highlight the importance of characterizing the corresponding histopathological alterations in experimental models.

Evidence also suggests a potential relationship between β-amyloid (Aβ) and male reproductive tissues. Exposure of human spermatozoa to Aβ *in vitro* adversely affected sperm motility and function [15]. Amyloid precursor protein (APP), the precursor from which Aβ peptides are generated, has also been identified in testicular tissue [16, 17]. These observations indicate that components of the amyloidogenic pathway are present within the male reproductive system and provide a biological basis for investigating Aβ-associated changes in testicular tissue. However, Aβ immunoreactivity should be distinguished from definitive biochemical identification of the deposited amyloid protein.

Although CasNa is an established experimental stimulus associated with chronic inflammatory responses and AA amyloid formation, previous experimental work has predominantly focused on systemic AA amyloidosis and increased SAA production [18]. Consequently, the pathological effects of prolonged CasNa administration on the testis remain poorly characterized. Specifically, whether CasNa-associated testicular lesions are accompanied by progressive amyloid deposition and increased Aβ immunoreactivity remains poorly investigated. This gap is particularly relevant because APP has been demonstrated in human and rat testes [19], while chronic inflammation and inflammatory mediators have been associated with altered APP expression and processing and increased Aβ accumulation in other tissues [20, 21]. Thus, integrated histopathological, histochemical, and immunohistochemical characterization is required to determine the temporal progression of testicular lesions and amyloid-associated changes following CasNa administration.

Therefore, this study aimed to investigate the development and progression of testicular amyloidosis in adult male rats following intraperitoneal (IP) administration of CasNa at different experimental time points. Specifically, the study evaluated CasNa-associated changes in testicular histoarchitecture and seminiferous tubule morphology, characterized amyloid deposition using Congo red staining, and assessed Aβ immunoreactivity using immunohistochemistry (IHC). By integrating histopathological, histochemical, histomorphometric, and immunohistochemical assessments, the study sought to characterize the temporal progression of CasNa-associated testicular lesions and provide an experimental basis for further investigation of amyloid pathobiology in the male reproductive system.

MATERIALS AND METHODS

Ethical approval

The study protocol was reviewed and approved by the Institutional Animal Care and Use Committee of the

College of Veterinary Medicine, University of Mosul, Mosul, Iraq, on October 15, 2024 (approval no. UM.VET.2024.161). All procedures involving adult male Albino Wistar rats (*Rattus norvegicus*), including animal housing, acclimatization, IP administration of the experimental treatments, monitoring, euthanasia, and tissue collection, were conducted in accordance with the approved institutional protocol and the ARRIVE 2.0 guidelines. Animals were maintained under controlled laboratory conditions with free access to food and water, and appropriate measures were taken throughout the experimental period to minimize unnecessary discomfort and distress. Animal welfare was monitored throughout the experiment by assessing general health and behavior, and appropriate measures were taken to minimize pain, distress, and discomfort. Humane endpoints were to be applied in accordance with the approved institutional protocol when necessary.

Study period and location

The experiment was conducted for 60 days, from 20/10/2024 to 8/1/2025, at the Animal Unit, College of Veterinary Medicine, University of Mosul, Mosul, Iraq.

Animals

Twenty healthy adult male Albino Wistar rats (*R. norvegicus*), aged 2 months and weighing 250–300 g, were obtained from the Animal Unit, University of Mosul. Before the experiment, all animals were acclimatized for 2 weeks. The rats were housed in clean plastic cages under standard laboratory conditions at 22 ± 2°C with a 12-h light/12-h dark cycle. Food and water were provided *ad libitum* throughout the experimental period.

Study design

Twenty rats were randomly allocated to two groups of 10 animals each using a simple lottery method. The control group received IP injections of 3.0 mL/kg distilled water, whereas the treatment group received IP injections of 8% (w/v) CasNa (Sigma-Aldrich, USA, Catalog no. C8654) at 3.0 mL/kg body weight, based on a previously described protocol [22]. CasNa solution was prepared by dissolving the powder in distilled water and continuously stirring for 4 h at room temperature [23]. Before administration, the pH was adjusted to 7.0–7.4, and each freshly prepared batch was filtered through a 0.22-µm syringe filter (Sigma-Aldrich).

The injection schedule of control and treatment groups consisted of four consecutive days of administration followed by 1 day without injection, with this schedule applied throughout the experimental period. All rats remained clinically normal, and no infections or mortality were observed during the study.

Animals were evaluated at two experimental time points. On day 25, five animals from each group were euthanized, with the selection of this time point based on a previous study [7]. On day 60, the remaining five animals from each group were euthanized. Before euthanasia, animals were anesthetized by injection of ketamine and xylazine, followed by cervical dislocation. Testes were subsequently collected and fixed in 10% neutral-buffered formalin at room temperature for histopathological and histochemical examinations [24].

Histopathological examination

Testicular tissues were fixed in 10% neutral-buffered formalin for at least 48 h and subsequently rinsed under running water. The samples were dehydrated through graded ethanol concentrations, beginning with 70% ethanol overnight, followed by 80% ethanol for 1 h, two changes of 90% ethanol for 1 h each, and two changes of absolute ethanol for 1 h each. The tissues were then cleared in two changes of xylene for 30 min each and infiltrated with molten paraffin wax at 55–58°C using three consecutive changes of 1 h each.

The tissues were oriented in paraffin molds and allowed to solidify at room temperature (22–25°C). Paraffin blocks were sectioned at a thickness of 5 µm using a rotary microtome. Sections were stained with hematoxylin and eosin (H&E) and examined using light microscopy [25]. Amyloid-associated deposits were assessed using Congo red staining according to the method described previously [26]. Histopathological examinations were performed independently and blindly by two experienced pathologists. Slides were assigned coded identification numbers to conceal treatment group allocation and experimental time points.

Histomorphometric analysis

Histomorphometric analysis was performed to evaluate differences in seminiferous tubule diameter among the experimental groups. One testicular slide from each animal was evaluated. Five microscopic fields were randomly selected from each slide, and five seminiferous tubules were measured within each field, yielding 25 tubule measurements per animal. Tubule-level measurements were averaged to obtain a single mean value for each animal, and the individual animal was considered the experimental unit (n = 5/group at each time point).

Images were acquired at 40× magnification using an OMAX A35180U3 camera (China) connected to an Olympus microscope (Japan). Seminiferous tubule diameters were measured using ToupView software (OMAX, China) [27].

Immunohistochemical examination and validation

IHC was performed to assess Aβ immunoreactivity in testicular tissue. Paraffin-embedded tissues were sectioned at 5 µm using a rotary microtome and mounted on positively charged slides. Sections were deparaffinized in xylene and rehydrated through descending concentrations of ethanol. Heat-induced epitope retrieval was performed by immersing the slides in citrate buffer (pH 6.0) and heating them in a microwave at 95°C for 10 min. The slides were subsequently cooled at room temperature for 20 min and washed three times with phosphate-buffered saline (PBS; pH 7.4).

Endogenous peroxidase activity was blocked using hydrogen peroxide (H_2O_2), followed by blocking of nonspecific protein binding with goat serum. Sections were incubated with a rabbit polyclonal anti-Aβ primary antibody (1:100; Elabscience, catalog no. E-AB-15509), followed by a goat anti-rabbit IgG secondary antibody (1:400; Wuhan Fine Biotech, China) for 30 min. Immunoreactivity was visualized using diaminobenzidine (DAB), and sections were counterstained with hematoxylin [28]. For the negative control, sections were incubated with normal rabbit IgG isotype instead of the primary antibody.

All slides were examined using an OMAX A35180U3 digital camera (China) connected to an Olympus microscope (Japan). Five fields at 40× magnification were assessed from each of five slides per experimental time point by two pathologists, and the mean Aβ immunoreactivity score was calculated from the evaluated fields for each group; images were analyzed using ImageJ Fiji version 2.14.0 (USA) to evaluate Aβ immunoreactivity based on staining intensity [29].

Statistical analysis

Histomorphometric and immunohistochemical data were expressed as mean ± standard error of the mean (SEM). Data normality was assessed using the Shapiro–Wilk test. Differences among groups were evaluated using one-way analysis of variance, followed by Tukey's post hoc test for multiple comparisons. Statistical analyses were performed using GraphPad Prism version 10.2.0 (GraphPad Software, USA). Statistical significance was set at $p \leq 0.05$ [30].

RESULTS

Histopathological changes in the testes using H&E

After 25 days of treatment with 8% CasNa, testicular tissue showed alterations in the size and shape of some seminiferous tubules, vascular congestion and vasculitis, detachment of the germinal epithelium from the basement membrane, cessation of spermatogenesis, thickening of the basement membrane in some seminiferous tubules, and deposition of homogeneous eosinophilic proteinaceous material in the interstitial tissue (Figures 1C and D). In contrast, the control group showed normal testicular architecture, with seminiferous tubules exhibiting different stages of spermatogenesis (Figures 1A and B).

By day 60, the treatment group showed more extensive histopathological alterations, including severe necrosis of the seminiferous tubules, loss of normal testicular architecture and histological features, deposition of proteinaceous material, and mononuclear inflammatory cell infiltration (Figures 2A and B).

Histomorphometric measurement

Histomorphometric analysis revealed significant differences in seminiferous tubule diameter among the experimental groups ($p < 0.0001$). Seminiferous tubule diameter was significantly lower in the treatment group on day 25 (301.7 ± 4.597) than in the control group. A further significant decrease was observed in the treatment group on day 60 (241.4 ± 9.664) compared with both the day-25 treatment group and the control group (Figure 3).

Histopathological changes in the testes using Congo red staining

Congo red-stained testicular sections from the treatment groups on days 25 and 60 showed amyloid-associated deposits in testicular tissue. The deposits appeared as amorphous, homogeneous, extracellular orange-red material and were predominantly distributed in the interstitial tissue between the seminiferous tubules and along their basement membranes. The deposits were associated with distortion and narrowing of adjacent seminiferous tubules (Figure 4).

doi: 10.14202/vetworld.2026.4970-4980

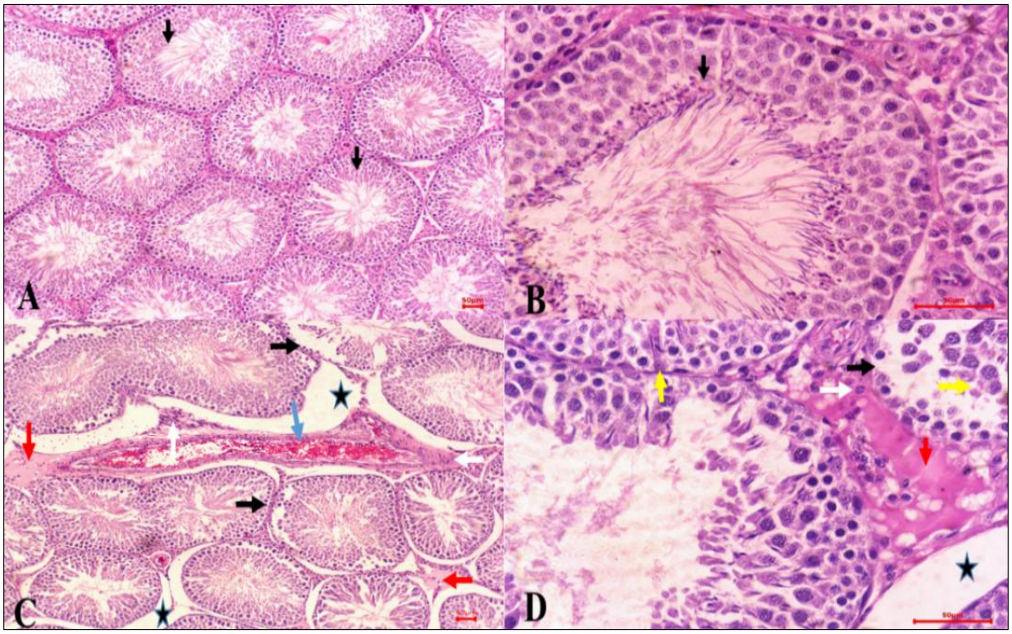


Figure 1: Histopathological findings in the testes stained with hematoxylin and eosin. (A and B) Control group showing normal histological architecture with numerous seminiferous tubules at different stages of spermatogenesis (black arrows). (C and D) Treatment group on day 25 showing vascular congestion (blue arrow), edema (black star), proteinaceous deposits (red arrows), germinal epithelial detachment (black arrows), inflammatory cell infiltration (white arrow), and spermatocyte degeneration (yellow arrow). Scale bar = 50 µm.

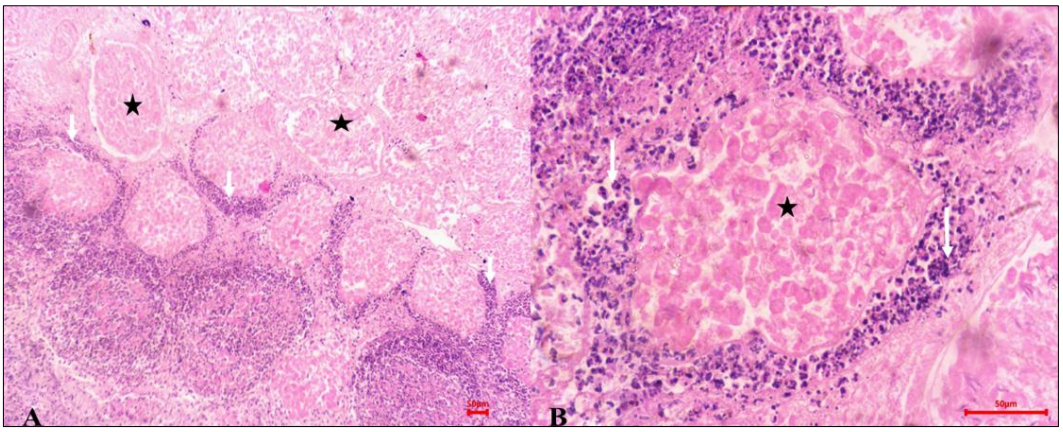


Figure 2: Histopathological findings in the testes stained with hematoxylin and eosin. (A and B) Treatment group on day 60 showing necrosis of the seminiferous tubules (black stars), deposition of homogeneous proteinaceous material, and mononuclear inflammatory cell infiltration (white arrows). Scale bar = 50 µm.

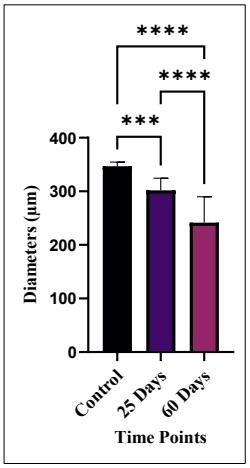


Figure 3: Seminiferous tubule diameter in the experimental groups. Error bars represent the standard error of the mean. Asterisks indicate significant differences between groups. SEM = standard error of the mean (Asterisks of *** indicate statistical differences at 0.001 and **** indicate statistical differences at 0.0001).

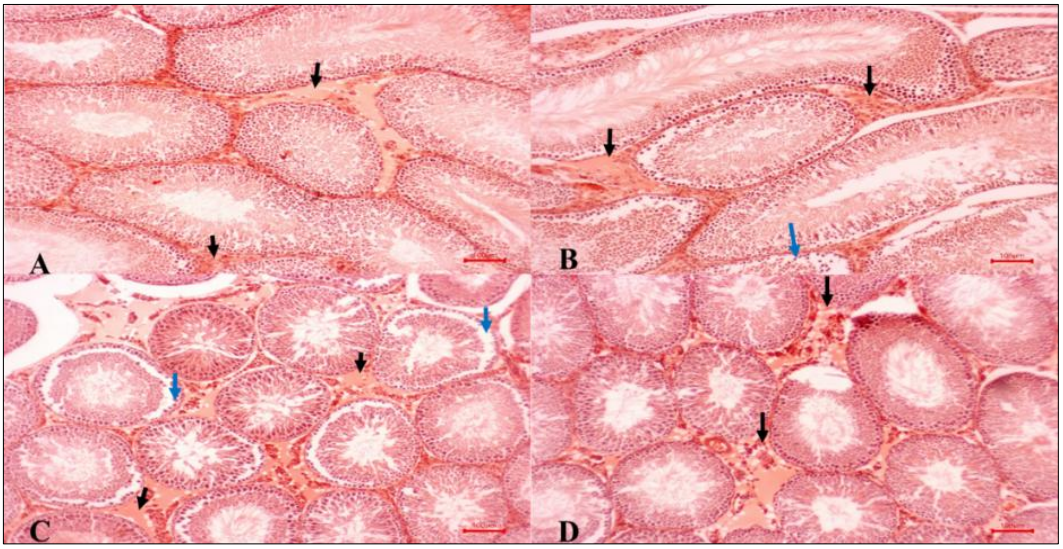


Figure 4: Histopathological findings in the testes of the treatment groups stained with Congo red. (A and B) Testicular tissue on day 25. (C and D) Testicular tissue on day 60. Amyloid-associated deposits are present between the seminiferous tubules (black arrows), with germinal epithelial detachment (blue arrows). Scale bar = 100 µm.

Aβ immunoreactivity in the testes

IHC was performed to assess Aβ immunoreactivity in testicular tissue. No Aβ immunoreactivity was observed in the control group (Figure 5A). In contrast, the treatment groups showed positive Aβ immunoreactivity, predominantly within the interstitial tissue between the seminiferous tubules. Staining intensity increased with treatment duration, progressing from moderate immunoreactivity on day 25 (30.42 ± 6.870) (Figures 5B and 6A) to intense immunoreactivity on day 60 (61.34 ± 6.870) (Figures 5C and 6B).

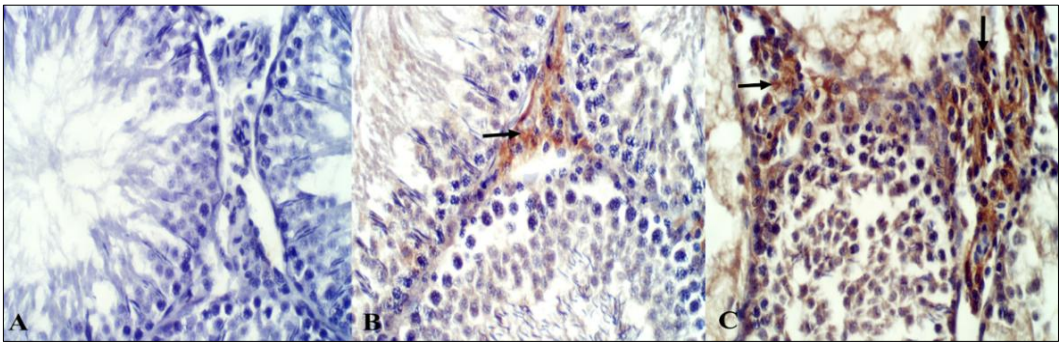


Figure 5: Immunohistochemical examination of β-amyloid immunoreactivity in the testes at high magnification. (A) Control group showing no interstitial immunoreactivity. (B) Treatment group showing moderate interstitial immunoreactivity on day 25. (C) Treatment group showing intense interstitial immunoreactivity on day 60. Black arrows indicate positive β-amyloid immunoreactivity. Magnification = 400×.

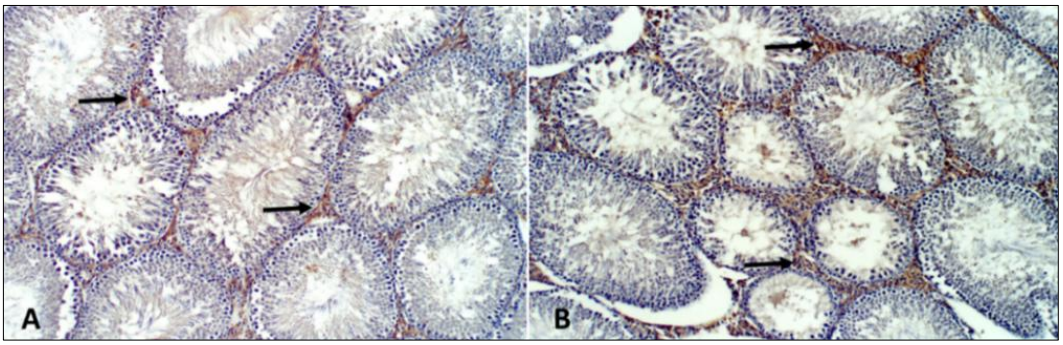


Figure 6: Immunohistochemical examination of β-amyloid immunoreactivity in the testes at low magnification. (A) Treatment group showing moderate interstitial immunoreactivity on day 25. (B) Treatment group showing intense interstitial immunoreactivity on day 60 (black arrows). Magnification = 100×.

The intensity of Aβ immunoreactivity differed significantly among the experimental groups ($p < 0.0001$). Both treatment groups showed significantly greater immunoreactivity than the control group, and intensity on day 60

was significantly higher than on day 25 (Figure 7). These findings showed a progressive increase in Aβ immunoreactivity as treatment duration increased.

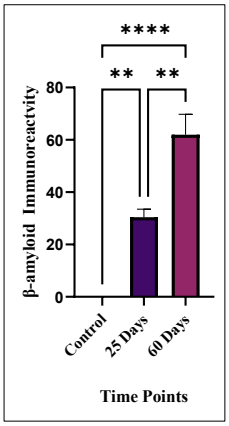


Figure 7: β-amyloid immunoreactivity in the testes assessed using IHC. Error bars represent the standard error of the mean. Asterisks indicate significant differences between groups. IHC = immunohistochemistry; SEM = standard error of the mean (Asterisks of ** indicate statistical differences at 0.01 and *** indicate statistical differences at 0.001).

DISCUSSION

Testicular histopathological changes and amyloid deposition

This study demonstrated progressive histopathological alterations in the testes of male rats treated with CasNa, accompanied by amyloid-associated deposition predominantly in the interstitial tissue. Amyloid formation generally involves abnormal folding of normally soluble precursor proteins, converting them into insoluble fibrillar aggregates characterized by a β-pleated sheet configuration [31, 32]. These fibrils accumulate predominantly in extracellular and interstitial compartments, where progressive deposition can disrupt tissue architecture and exert pressure on adjacent cells. Continued accumulation may consequently compromise the structural integrity and physiological function of affected organs [33, 34].

These findings align with previous evidence linking amyloid deposition to tissue damage in several organs, including the heart [35], lungs [36], and kidneys [37]. Importantly, experimental evidence also supports the susceptibility of male reproductive tissues to amyloid-associated injury. Ukwenya *et al.* [38] demonstrated amyloid deposition accompanied by histological and functional alterations in the testes and epididymides of a fructose-streptozotocin-induced model of type 2 diabetes. Similarly, Gonzalez *et al.* [39] reported interstitial testicular amyloid deposition, associated testicular atrophy, and pathological alterations in hamsters experimentally infected with *Leishmania donovani*. Other studies have further documented an association between amyloidosis and impaired testicular function [13, 40].

In the present study, CasNa treatment was associated with progressive structural alterations, including changes in seminiferous tubule morphology, germinal epithelial detachment, inflammatory changes, proteinaceous deposition, and severe testicular damage at the later experimental time point. The concomitant reduction in seminiferous tubule diameter further supports the progressive nature of these structural alterations. Although cessation of spermatogenesis was observed histologically, sperm characteristics, reproductive hormone concentrations, and fertility were not directly evaluated. Therefore, the present findings cannot establish the functional reproductive consequences of these histopathological alterations.

Aβ immunoreactivity in testicular tissue

IHC examination showed Aβ immunoreactivity in testicular tissue from CasNa-treated rats, with staining intensity increasing from day 25 to day 60. Studies investigating Aβ in the male reproductive system remain limited because most previous research has focused on its involvement in the central nervous system and its association with Alzheimer's disease [41–43]. Accumulation of Aβ in brain tissue is a prominent pathological feature of Alzheimer's disease and contributes to amyloid plaque formation associated with neurodegenerative changes [44, 45]. Nevertheless, Aβ-related proteins are not restricted to neural tissues. Roher *et al.* [46] demonstrated Aβ peptides in several peripheral tissues, including skeletal muscle, the aorta, and the liver.

The observed testicular Aβ immunoreactivity is also relevant to APP in the male reproductive system. Silva *et al.* [16] characterized an APP interaction network in human testicular tissue, while previous evidence has also demonstrated APP in the testis [19]. Because APP is the precursor to Aβ peptides, its presence provides a

biological basis for investigating amyloidogenic processes in testicular tissue. However, the current IHC findings demonstrate Aβ immunoreactivity rather than definitive biochemical identification of the deposited amyloid protein.

Potential relationship between inflammation and Aβ immunoreactivity

The mechanisms underlying the increased Aβ immunoreactivity observed following CasNa administration were not directly investigated in this study. Nevertheless, chronic inflammation has been associated with alterations in APP expression and processing and may promote Aβ accumulation in other tissues [21]. Because CasNa administration was accompanied by inflammatory histopathological changes in the present study, sustained inflammatory stimulation may be associated with the increased Aβ immunoreactivity observed in the testicular tissue. However, inflammatory mediators, APP expression, APP processing pathways, and Aβ concentrations were not directly measured. Therefore, a causal relationship between CasNa-induced inflammation and altered APP processing or Aβ production cannot be established from the present findings.

Interpretation of amyloid and Aβ findings

The combined histopathological, Congo red, and IHC findings provide complementary evidence of amyloid-associated pathological alterations in the testes following CasNa administration. Congo red staining demonstrated extracellular amyloid-associated deposits, whereas IHC demonstrated increased Aβ immunoreactivity in the treated groups. Importantly, these observations do not definitively show that the Congo red-positive material consists specifically of Aβ. Aβ immunoreactivity alone does not establish the biochemical identity of the deposited amyloid protein. Additional analytical approaches are therefore required to characterize the deposits and establish their molecular composition.

Strengths and limitations

A strength of the present study was the combined use of conventional histopathology, histomorphometric assessment, Congo red staining, and IHC to characterize testicular alterations at two experimental time points. This approach enabled evaluation of the temporal progression of structural changes, amyloid-associated deposition, and Aβ immunoreactivity following CasNa administration.

Several limitations should be considered when interpreting these findings. The relatively small sample size may limit the generalizability and statistical precision of the results. In addition, Congo red-stained sections were not examined using polarized light microscopy; therefore, characteristic apple-green birefringence was not demonstrated. The study also lacked biochemical or molecular confirmation of the identity of the deposited amyloid protein. Furthermore, testosterone concentrations, quantitative spermatogenic parameters, sperm quality, and fertility outcomes were not evaluated. Consequently, although the study demonstrated substantial histopathological alterations, it cannot determine their direct effects on reproductive function.

Future research

Further studies should incorporate complementary molecular and biochemical approaches to characterize the deposited amyloid protein and investigate the mechanisms underlying its accumulation in testicular tissue. Quantitative assessment of APP and Aβ, together with evaluation of relevant inflammatory and amyloidogenic pathways, could help clarify the relationship between CasNa-induced inflammatory responses and testicular amyloid-associated alterations. SDS-PAGE and other protein-characterization approaches may provide additional information; however, more specific amyloid typing methods, including mass spectrometry, would be valuable for determining the molecular identity of the deposits. Future studies should also assess reproductive hormones, quantitative spermatogenesis, sperm characteristics, and fertility outcomes to determine the functional consequences of testicular amyloid deposition.

CONCLUSION

Repeated CasNa administration was associated with progressive testicular amyloid-associated pathology in adult male rats. Histopathological examination demonstrated time-dependent alterations in testicular architecture, including seminiferous tubule damage, germinal epithelial detachment, inflammatory changes, interstitial proteinaceous deposition, and more extensive tissue injury by day 60. These alterations were accompanied by a progressive reduction in seminiferous tubule diameter. Congo red staining showed extracellular amyloid-associated deposits predominantly in the interstitial tissue and along the seminiferous tubule basement membranes. In addition, IHC showed greater Aβ immunoreactivity on day 60 than on day 25. However, Aβ

immunoreactivity alone does not establish that the Congo red-positive deposits consist specifically of Aβ.

The findings indicate that repeated CasNa administration makes the testis susceptible to amyloid-associated structural alterations. This experimental approach may therefore provide a useful basis for investigating the development and progression of testicular amyloid-associated pathology and its potential relationship with male reproductive tissue damage. However, these findings should not be interpreted as evidence of impaired fertility because we did not directly assess reproductive function.

In conclusion, repeated CasNa administration was associated with progressive testicular structural damage, Congo red-positive amyloid-associated deposition, and increased Aβ immunoreactivity in adult male rats. The findings provide an experimental basis for further investigation of amyloid-associated pathology in the male reproductive system. Nevertheless, definitively identifying the deposited amyloid protein and determining its effects on reproductive function require additional molecular, biochemical, and functional studies.

DATA AVAILABILITY

The data supporting the findings of this study are available within the manuscript.

GENERATIVE AI DECLARATION

The authors acknowledge that generative AI was used solely for language improvement and was not used for data analysis or interpretation of the study results.

AUTHORS' CONTRIBUTIONS

MAA and SHA: Conceptualized and designed the study, conducted the experiment, collected tissue samples, performed histological processing and IHC, and drafted the manuscript. AMA and HKI: Performed the microscopic examination and IHC validation and assessment. SHA: Performed the statistical analysis and interpreted the results. All authors have read and approved the final version of the manuscript.

ACKNOWLEDGMENTS

The authors thank the technical staff of the Department of Pathology and Poultry Diseases at the Veterinary Teaching Hospital, College of Veterinary Medicine, and the Animal Unit, University of Mosul, Mosul, Iraq, for their technical assistance and support during the study. This study received no external funding and was self-funded by the authors.

COMPETING INTERESTS

The authors declare that they have no competing interests.

PUBLISHER'S NOTE

Veterinary World remains neutral with regard to jurisdictional claims in the published institutional affiliations.

REFERENCES

1. Al-Ameen S, Mohammed R. Clinical features, diagnosis and treatment of amyloidosis: a review. JLBSR. 2024;5(01):08–12.
2. Musetti V, Greco F, Aimo A, Castiglione V, Vergaro G, Panichella G, *et al*. Cardiac amyloidosis: role of the endomyocardial biopsy. Heart Fail Clin. 2024;20(3):e23–31.
3. Nakamura K. Molecular research on amyloidosis. Int J Mol Sci. 2023;24(8):6980.
4. Adrogue HE. Amyloidosis of the heart and kidney. Methodist Debakey Cardiovasc J. 2022;18(4):27.
5. Rosenzweig M, Kastritis E. Liver and gastrointestinal involvement: update. Hematol Oncol Clin North Am. 2020;34(6):e1–3.
6. Chompoopong P, Mauermann ML, Siddiqi H, Peltier A. Amyloid neuropathy: from pathophysiology to treatment in light chain amyloidosis and hereditary transthyretin amyloidosis. Ann Neurol. 2024;96(3):423–440.
7. Skinner M, Shirahama T, Benson MD, Cohen AS. Murine amyloid protein AA in casein-induced experimental amyloidosis. Lab Invest. 1977;36(4):420–427.
8. Domínguez-Melendez V, Silvestre-Santana O, Moreno-Fierros L, Aguiñiga-Sánchez I, Martínez L, Marroquin-

Segura R, *et al*. Sodium caseinate induces mouse granulopoiesis. Inflamm Res. 2012;61(4):367–373.
9. Santiago-Osorio E, Ledesma-Martínez E, Aguiñiga-Sánchez I, Poblano-Pérez I, Weiss-Steider B, Montesinos-Montesinos JJ, *et al*. Sodium caseinate (CasNa) induces mobilization of hematopoietic stem cells in a BALB/c mouse model. Med Sci Monit Basic Res. 2015;21:206.
10. Merlini G, Bellotti V. Molecular mechanisms of amyloidosis. N Engl J Med. 2003;349(6):583–596.
11. Mirioglu S, Uludag O, Hurdogan O, Kumru G, Berke I, Doumas SA, *et al*. AA amyloidosis: a contemporary view. Curr Rheumatol Rep. 2024;26(7):248–259.
12. Buxbaum JN, Eisenberg DS, Fändrich M, McPhail ED, Merlini G, Saraiva MJ, *et al*. Amyloid nomenclature 2024: update, novel proteins, and recommendations by the International Society of Amyloidosis (ISA) Nomenclature Committee. Amyloid. 2024;31(4):249–256.
13. Delbarba A, Facondo P, Fisogni S, Izzi C, Maffezzoni F, Pezzaioli LC, *et al*. Testicular involvement is a hallmark of Apo AI Leu75Pro mutation amyloidosis. J Clin Endocrinol Metab. 2020;105(12):e4758–4766.
14. Ozcan AK, Karaoglan B, Gundogdu B, Sahin C, Simsekoglu MF, Ugurlu S. Urological manifestations in familial Mediterranean fever excluding renal amyloidosis: a systematic review. Rheumatology. 2026;65(5):keag127.
15. Tavares RS, Martins S, Almeida-Santos T, Sousa AP, Ramalho-Santos J, Da Cruz e Silva OA. Alzheimer's disease-related amyloid-β1–42 peptide induces the loss of human sperm function. Cell Tissue Res. 2017;369(3):647–651.
16. Silva JV, Yoon S, Domingues S, Guimarães S, Goltsev AV, da Cruz e Silva EF, *et al*. Amyloid precursor protein interaction network in human testis: sentinel proteins for male reproduction. BMC Bioinformatics. 2015;16(1):12.
17. Seyedreza P, Alireza MN, Seyedebrahim H. Role of testosterone in memory impairment of Alzheimer disease induced by streptozotocin in male rats. DARU. 2012;20(1):98.
18. Eriksen N, Ericsson LH, Pearsall N, Lagunoff D, Benditt EP. Mouse amyloid protein AA: homology with nonimmunoglobulin protein of human and monkey amyloid substance. Proc Natl Acad Sci U S A. 1976;73(3):964–967.
19. Shoji MI, Kawarabayashi T, Harigaya Y, Yamaguchi H, Hirai S, Kamimura T, *et al*. Alzheimer amyloid beta-protein precursor in sperm development. Am J Pathol. 1990;137(5):1027.
20. Schmidt J, Barthel K, Wrede A, Salajegheh M, Bähr M, Dalakas MC. Interrelation of inflammation and APP in sIBM: IL-1β induces accumulation of β-amyloid in skeletal muscle. Brain. 2008;131(5):1228–1240.
21. Cipriano GL, Anchesi I, Raffaele I, Astorino MF, Minuti A, Calabrò M, *et al*. Neuroinflammation and secretase regulation in Alzheimer's disease: from molecular cross-talk to multi-target therapeutics. Int J Mol Sci. 2026;27(11):4824.
22. Ramos G, Weiss B, Córdova Y, Hernández J, Zambrano I, Santiago E. Sodium caseinate induces expression and secretion of murine multipotent myeloid cell line 32D macrophage colony-stimulating factor. Arch Med Res. 2004;35(2):109–113.
23. Valentino M, Volpe S, Di Giuseppe FA, Cavella S, Torrieri E. Active biopolymer coating based on sodium caseinate: physical characterization and antioxidant activity. Coatings. 2020;10(8):706.
24. Tian P, Yang Z, Qu C, Qi X, Zhu L, Hao G, *et al*. Exploration of tissue fixation methods suitable for digital pathological studies of the testis. Eur J Med Res. 2024;29(1):319.
25. Luna LG. Manual of histologic staining methods of the Armed Forces Institute of Pathology. 3rd ed. New York: McGraw-Hill; 1968.
26. Bancroft JD, Layton C. Connective and other mesenchymal tissues with their stains. In: Bancroft's theory and practice of histological techniques. 2018. p. 153.
27. Altaey OY, Hasan AA, Alhaaik AG. Early-life development of spleen in white rabbit (*Oryctolagus cuniculus*): a morphometric and histochemical analysis. Vet Integr Sci. 2025;23(1):e2025012-1-13.
28. Mebratie DY, Dagnaw GG. Review of immunohistochemistry techniques: applications, current status, and future perspectives. Semin Diagn Pathol. 2024;41(3):154–160.
29. Aho L, Pikkarainen M, Hiltunen M, Leinonen V, Alafuzoff I. Immunohistochemical visualization of amyloid-β protein precursor and amyloid-β in extra- and intracellular compartments in the human brain. J Alzheimers Dis. 2010;20(4):1015–1028.
30. Panos GD, Boeckler FM. Statistical analysis in clinical and experimental medical research: simplified guidance for authors and reviewers. Drug Des Devel Ther. 2023;17:1959–1961.
31. Salzillo C, Franco R, Ronchi A, Quaranta A, Marzullo A. Cardiac amyloidosis: state-of-the-art review in

molecular pathology. Curr Issues Mol Biol. 2024;46(10):11519–11536.
32. Aydin I, Kursun AS, Gunboz M, Okumus SY, Unverengil GG, Emel E. Dural amyloidoma located in the falx cerebri and spinal dura: two case reports. Turk Neurosurg. 2026;36(1).
33. Merlini G, Dispenzieri A, Sanchorawala V, Schönland SO, Palladini G, Hawkins PN, *et al*. Systemic immunoglobulin light chain amyloidosis. Nat Rev Dis Primers. 2018;4(1):38.
34. Sanchorawala V. Systemic light chain amyloidosis. N Engl J Med. 2024;390(24):2295–2307.
35. Kanj F, Kara D, Wexler E, Garrett T, Mai D, Hanna M, *et al*. Cardiac diffusion tensor imaging may detect early cardiac amyloidosis in carpal tunnel syndrome. JACC Adv. 2026;5(2):102562.
36. Khoor A, Colby TV. Amyloidosis of the lung. Arch Pathol Lab Med. 2017;141(2):247–254.
37. Gurung R, Li T. Renal amyloidosis: presentation, diagnosis, and management. Am J Med. 2022;135:S38–S43.
38. Ukwenya VO, Aderemi AS, Alese OM, Augustine OA. Caffeic acid abrogates amyloidosis, hypospermatogenesis and cell membrane alterations in the testes and epididymis of fructose-diabetic rats by upregulating steroidogenesis, PCNA and Nrf2 expression. Tissue Cell. 2022;79:101912.
39. Gonzalez JL, Gallego E, Castaño M, Rueda A. Testicular amyloidosis in hamsters experimentally infected with *Leishmania donovani*. Br J Exp Pathol. 1983;64(5):518.
40. Scalvini T, Martini PR, Gambera A, Tardanico R, Biasi L, Scolari F, *et al*. Spermatogenic and steroidogenic impairment of the testicle characterizes the hereditary leucine-75-proline apolipoprotein A-I amyloidosis. J Clin Endocrinol Metab. 2008;93(5):1850–1853.
41. Zhang H, Zheng Y. β amyloid hypothesis in Alzheimer's disease: pathogenesis, prevention, and management. Acta Acad Med Sin. 2019;41(5):702–708.
42. Jin Y, Du Q, Song M, Kang R, Zhou J, Zhang H, *et al*. Amyloid-β-targeting immunotherapies for Alzheimer's disease. J Control Release. 2024;375:346–365.
43. Shahsavari F, Eidi A, Sotoodehnejadnematalahi F. Neuroprotective effects of sodium molybdate in a beta-amyloid–induced rat model of Alzheimer's disease: an *in vivo* preclinical study. J Trace Elem Med Biol. 2025:127774.
44. Zhang B, Li Y, Li H, Shen X, Zhu Z. Therapeutic advances in targeting the amyloid-β pathway for Alzheimer's disease. Brain Sci. 2025;15(10):1101.
45. Karati D, Mukherjee S, Roy S. The antioxidant potential of bacoside and its derivatives in Alzheimer's disease: the molecular mechanistic paths and therapeutic prospects. Toxicol Rep. 2025;14:101945.
46. Roher AE, Esh CL, Kokjohn TA, Castaño EM, Van Vickle GD, Kalback WM, *et al*. Amyloid beta peptides in human plasma and tissues and their significance for Alzheimer's disease. Alzheimers Dement. 2009;5(1):18–29.

****